

# Predicting Exotic Hadron Masses with Data Augmentation Using Multilayer Perceptron

Huseyin Bahtiyar<sup>1</sup>

<sup>1</sup>*Department of Physics, Faculty of Science and Letters,  
Mimar Sinan Fine Arts University, Bomonti 34380, Istanbul, Turkey*

(Dated: August 23, 2022)

Recently, there have been significant developments in neural networks; thus, neural networks have been frequently used in the physics literature. This work estimates the masses of exotic hadrons, doubly charmed and bottomed baryons from the meson and baryon masses using neural networks. Subsequently, the number of data has been increased using the artificial data augmentation technique proposed recently. We have observed that the neural network's predictive ability increases using augmented data. This study has shown that data augmentation techniques play an essential role in improving neural network predictions; moreover, neural networks can make reasonable predictions for exotic hadrons, doubly charmed, and doubly bottomed baryons. The results are also comparable to Gaussian Process and Constituent Quark Model.

Keywords: Neural Networks; Hadron Mass; Charmed and Bottomed Baryons.

## I. INTRODUCTION

The mass is a fundamental feature of hadrons, which provides information about the strong interaction. The bare masses of the valence quark (or anti-quark) in hadrons are very small compared to the hadron's effective mass, so most of the mass of matter around us results from strong interaction. The precise mass predictions, either experimentally or theoretically, help us understand the theories better and develop the models.

Quantum chromodynamics (QCD) is the fundamental quantum field theory of strong interaction, which confines quarks, anti-quarks, and gluons. In QCD, there are six different quark flavors, up ( $u$ ), down ( $d$ ), strange ( $s$ ), charm ( $c$ ), beauty ( $b$ ) and top ( $t$ ). Also there are three color states, represented by red ( $r$ ), green ( $g$ ) and blue ( $b$ ). In QCD, quarks carry color, anti-quarks carry anti-color, and gluons carry one color and one anti-color. Thus, quarks and anti-quarks have three color states, and gluons have eight different combinations of color states. Peculiarly, a single quark with a color charge could not be observed by experiments. According to the color confinement phenomenon, color-charged particles cannot be isolated and cannot be directly observed or measured.

Consequently, only color singlet particles are observable in experiments. QCD describes quark and gluon dynamics successfully in large momentum transfer interactions. In the high energy regime, the coupling constant of strong interaction is small, and perturbation theory is applicable. On the other hand, in the low energy regime, the strong coupling constant is dominant and perturbative methods cannot be applied.

Since quarks and gluons, the elementary particles of the strong interaction, have not been observed as isolated particles, it is believed that the color potential between the quarks and gluons is responsible for such a mechanism and forms the color singlet objects called mesons ( $q\bar{q}$ ) and baryons ( $qqq$ ).

Exotic hadrons have structure other than conventional  $q\bar{q}, qqq$  configuration. A misinterpreted fact is that their possibility was declared as the quark model proposed. Exotics usually have several types of forms; the multi-quark form, such as tetraquark ( $qq\bar{q}\bar{q}$ ), pentaquark ( $qqqq\bar{q}$ ), which are formed from the same quark-level interactions as ordinary hadrons. The hadronic molecule is bound via meson exchange, and they are a composite form of the ordinary hadrons. Hybrid hadrons are formed as gluonic excitation of valence quarks which can be found with unconventional quantum numbers. These exotic hadrons are also color singlets, which are allowed by QCD.

Thanks to the developments in experimental facilities, producing heavy hadrons and composite particles are possible. The first exotic particle was reported in  $B^\pm \rightarrow J/\psi\pi^+\pi^-K^\pm$  channel by BELLE experiment in 2003 [1]. The X(3872) was estimated to contain four quarks and the quark structure is  $c\bar{c}\ell\bar{\ell}$ . Investigation of X(3872) has been continued and detailed analyzes were made by different experiments [2–4], finally in 2013 LHCb collaboration performed an amplitude analysis and quantum number was assigned as  $J^{PC} = 1^{++}$  [5]. Afterward, more four quark type hadrons have been observed in the charm quark sector, such as  $Z_c$  [6] and  $Z_b$  in the bottom quark sector [7]. Recently, in LHC, pentaquark structures have also been observed [8]. Theoretical studies such as the QCD sum rules and Lattice QCD try to shed some light on the internal structure of these observed particles.

Recently, there has been a significant interest in machine learning and its applications in physics. neural networks has proven itself making successful predictions in nuclear physics [9–12], and particle physics [13–17]. Also they are useful tools when solving differential equations [18–20]. In Lattice QCD, neural networks are used and active studies are carried out to reduce the use of intensive computer power [21–23].

It is known that neural networks generally perform better, and their generalization ability enhances as the training data increases [24–26]. Predicting masses of hadrons using neural networks is challenging since the number of experimentally observed hadrons is limited. Recently, a similar study was carried out for binding energies in nuclear physics [12] later, and a data augmentation technique was developed to improve the results [27]. In light of these developments, the masses of exotic particles are predicted by using the experimental masses of meson and baryon with a similar data augmentation technique.

This paper is organized as follows: Implementation of particle data and detailed information on the neural network architectures are given in Section II. In Section III, the results are presented and compared with other works. Finally, we discuss our findings in Section IV.

## II. NEURAL NETWORKS AND EXPERIMENTAL SETUP

This work aims to build a model that makes mass predictions for exotic hadrons using the quantum numbers and charge as inputs. The model takes these properties as an input and predicts the masses as an output. Such problems, where the outcome is a numerical value, are called the *regression* problems, which is a supervised learning problems. The aim is to learn the mapping from the input to the output. Multilayer perceptron (MLP), an architecture mainly favored for unraveling such regression problems, is chosen as the model for this work.

The aim of the supervised neural networks is to teach the model to map inputs to outputs from the training dataset. The structure of the neural network is built by layers. The first layer is the input layer, and the last layer is the output layer. The layers in between are called hidden layers. Each layer contains a certain number of neurons connected by a weight that provides information about neurons' importance. The value of a neuron is calculated by multiplying and summing the inputs with the weights. Then, the weighted sum is inserted into an activation function as given in Equations (1) and (2) which are generally chosen as non-linear functions. Every hidden layer takes the activation of its preceding layer as input, and this calculation propagates in the forward direction. After completing the forward pass, an error is computed using a loss function. The weights are updated in the backward pass using the error.

$$h_n^{(1)} = a \left( \mathbf{w}_n^{(1)T} \mathbf{x} \right) = a \left( \sum_{i=0}^d w_{ni}^{(1)} x_i + w_{n0}^{(1)} \right), n = 1 \dots H_1 \quad (1)$$

$$h_l^{(2)} = a \left( \mathbf{w}_l^{(2)T} \mathbf{h}^{(1)} \right) = a \left( \sum_{n=0}^{H_1} w_{ln}^{(2)} h_n^{(1)} + w_{l n_0}^{(2)} \right), l = 1 \dots H_2 \quad (2)$$

$$y = \mathbf{v}^T \mathbf{h}^{(2)} = \sum_{l=1}^{H_2} v_l h_l^{(2)} + v_0 \quad (3)$$

While designing a model for a supervised machine learning problem, the user must decide the algorithms or techniques to bring along some parameters. At the beginning of the problem, it is unclear which preference to make for these parameters. The selection of the parameters varies according to the problem itself or the given dataset. Parameters that are called *hyperparameters*, left to the user's choice, vary according to the problem and data set. Choosing the most appropriate hyperparameter group is one of the crucial problems in deep learning.

In neural networks, the learning process is basically an optimization problem; thus, optimization methods are used to find the optimum value in nonlinear problems. Different *optimization algorithms* are used in the literature. There are differences between these algorithms in terms of performance and speed. Therefore, the optimization algorithm is a hyperparameter that the user needs to choose. Another hyperparameter is called the *batch size*. The data set is divided into parts of batch size, and the model's training is done on this part in each iteration. Random selection of data in batch selection reduces overfitting. While the model is being trained, not all the data are included simultaneously. They take part in training in a certain number of pieces. The first piece is trained, the model's performance is tested, and the weights are updated according to the success with backpropagation. Then the model is retrained with the new training set, and the weights are updated again. This process is repeated at each training step to calculate the most appropriate weight values for the model. Each of these training steps is called an *epoch*. *Initialization of the weights* affects the learning and speed of the model. There are various ways to initialize the weight values. Therefore, the initialization of the weights is a hyperparameter. Differences in the scales across input variables may raise the problem's difficulty [28]. For instance, large input values may result in significant weight values, leading to the model suffering from poor performance during learning and producing higher generalization errors. Thus, *preprocessing* is another hyperparameter of the model. As a rule of thumb, input variables should be small values, usually between 0 – 1. *Activation functions* are used for nonlinear transformation operations in neural networks. The output of the

hidden layer is normalized with an activation function to calculate gradient descent. Finally, *the depth* of the model and *the number of neurons* in the hidden layers are also hyperparameters that the user must determine.

In addition to the list above, implementing data to the neural network might be regarded as a hyperparameter since it affects the model's performance. It is essential to correctly build the input layer, especially for physics data with many variables.

### A. Preprocessing the particle data

Neural networks are the structure that optimizes the output data from the input data. The previous section states that the model's performance depends on many different hyperparameters. The first hyperparameter is the preprocessing of the data. The meson and baryon data have been taken from Particle Data Group (PDG) [29] using python's Particle package [30]. The data contains the quark structure of hadron, isospin (I), angular momentum (J), parity (P) quantum numbers, and lastly, charge (Q) and the mass of the particle. The  $P$  quantum number is only taken  $-1$  or  $1$  values. I and J are positive half-integers; furthermore, the charge of the hadron is a float value.

Some of the particles have the same quark content, and quantum numbers but different mass; a neural network might have encountered difficulties while making a prediction; therefore, another variable called *state* (S) is introduced as proposed in Ref.[31]. This variable is ordered to rank them by their masses using the state value as the distinctive feature for the unclear inputs. Moreover, hadrons contain quarks/anti-quarks with six different flavors. Therefore data can be preprocessed in various ways. In this work, three different preprocess types were applied to the particle data gathered from the PDG.

In the first type, quarks inside the hadrons are separated into two labels as quarks ( $q$ ) and anti-quarks ( $\bar{q}$ ). These labels are filled with a mass of the bare quark value in units of MeV taken from PDG. In the first type, the input layer has 7 nodes as given in Equation (4). For the positively charged pion quark structure is one up and one anti-down quark  $\pi^+ = u\bar{d}$ , encoding the pion into a neural network is given in Equation (5).

$$\text{input}_7 = (q, \bar{q}, P, J, I, Q, S) \quad (4)$$

$$\pi^+ = (2.16, 4.67, 0, 0, 1, 1, 0) \quad (5)$$

The quarks inside the hadrons are labeled via quarks, anti-quarks, and their generation as  $q_1, \bar{q}_1, q_2, \bar{q}_2, q_3, \bar{q}_3$  for the second preprocessing. The first generation ( $q_1, \bar{q}_1$ ) contains up and down quarks, the second generation ( $q_2, \bar{q}_2$ ) is strange and charm quarks, lastly, flavors of the third generation ( $q_3, \bar{q}_3$ ) are bottom and top quarks. These labels are also filled with masses of specific bare quarks. In the second preprocessing, the input layer has 11 nodes as given in Equation (6). Encoding the positively charged pion into a neural network is given as an example in Equation (7).

$$\text{input}_{11} = (q_1, \bar{q}_1, q_2, \bar{q}_2, q_3, \bar{q}_3, P, J, I, Q, S) \quad (6)$$

$$\pi^+ = (2.16, 4.67, 0, 0, 0, 0, 0, 0, 1, 1, 0) \quad (7)$$

The procedure is followed in the last preprocessing proposed in Ref.[31]. In this technique, all quarks and anti-quarks are labeled separately; thus, filling with the bare quark masses will be redundant. For this reason, the labels are filled according to the number of quarks. Since no hadron containing top quark has been observed yet,  $t$  and  $\bar{t}$  labels are omitted, and the input layer has 15 nodes as given in Equation (8). Encoding the positively charged pion into a neural network is provided as an example in Equation (9).

$$\text{input}_{15} = (u, \bar{u}, d, \bar{d}, s, \bar{s}, c, \bar{c}, b, \bar{b}, P, J, I, Q, S) \quad (8)$$

$$\pi^+ = (1, 0, 0, 1, 0, 0, 0, 0, 0, 0, 0, 1, 1, 0) \quad (9)$$

Remaining hyperparameters and choices of the architectures will be explained in next section.

### B. Neural network architectures and Hyperparameters

A total of 432 meson and baryon masses have been obtained from PDG. Since the number of data is limited, one needs to consider the overfitting carefully. Thus, the input data is randomly divided into two subsets as 90.0% and 10.0% for training and test, respectively. Since this study aims to estimate the masses of exotic hadrons from the

experimental data taken from mesons and baryons, the test data is preserved as small as possible. Besides, the test data is used only to check whether there is overfitting. Overfitting occurs when training loss is larger than test loss; therefore, the loss values are carefully monitored. However, sometimes splitting the data as training and test set is not enough to avoid overfitting; different regularization methods could be used to overcome this problem, such as dropout, cross-validation, and regularization.  $L_2$  regularization is employed for hidden layers to avoid overfitting since the regularization is mainly used to penalize complex models in machine learning.

Another rule of thumb is that number of data should be more than the number of parameters in the model; this criterion needs to be considered when building the architectures. Total of 5 different architectures 16, 16 – 2, 16 – 4, 8 – 8 – 8 and 8 – 8 – 8 – 8 are implemented in this work. RMSProp, Adam, Adam with Nesterov momentum (NAdam), and another Adam based on optimizer Adamax are applied as optimizers. Mean Squared (MSE) and Mean Absolute errors (MAE) are implemented for losses. Glorot Normal and Glorot Uniform are preferred for weight initializers. Finally, for activation, ReLU and tanh functions are chosen. Epochs vary from 1000 to 5000 and batch sizes selected as 16, 32, 64. Artificial training data is obtained by adding random noise to the original input. Then, the original and artificial data are concatenated. In addition to avoiding overfitting, this technique improves the robustness of neural networks [32].

### C. Data augmentation

It is a known fact that the neural network performs better when the number of data increases. In our problem, the experimental data of the hadron masses is limited; in this manner, we tried to improve the estimations of the model by artificially increasing our data by following the prescription given in the reference [27].

Firstly, experimental errors are manually added, and the training data is doubled. Then, using the method specified in the reference [27], the training data is increased from 2 to 10 times using the normal distribution given in Equation (10). The Gaussian probability density function is defined as

$$f(x) = \frac{1}{\sqrt{2\pi}\sigma^2} \exp\left(-\frac{(x-\mu)^2}{2\sigma^2}\right) \quad (10)$$

where  $\mu$  and  $\sigma$  are the mean and the standard deviation, respectively, during the computations, the testing set remains constant, and only the data in the training set is artificially augmented. The increased data is stored every time and added to the next resample over the previous one. Therefore the fluctuation that comes from randomness is minimized.

## III. RESULTS

This study is aimed to predict the masses of exotic structured hadrons observed in experiments by giving the possible quantum numbers and charges as inputs. The neural networks have been trained using the experimental values of mesons and baryons. We try to predict hadrons with tetraquark structure X3872, Z3900, Z4200, Z4430, Y4260, Y4360, Y4660,  $Z_b(100610)$ ,  $Z_b(100650)$  and pentaquark hadrons  $P_c(4312)$ ,  $P_c(4440)$ ,  $P_c(4457)$  which recently observed by the LHCb experiment. Finally, we have estimated the masses of the baryons  $\Omega_{cc}$ ,  $\Omega_{cc}^*$ ,  $\Xi_{cc}^*$ ,  $\Omega_{bb}$ ,  $\Omega_{bb}^*$ ,  $\Xi_{bb}$ ,  $\Xi_{bb}^*$  predicted by theoretical studies but have not been observed by experiments yet.

The work begins with preprocessing the data; we implement three different input sizes 7, 11, and 15 as explained in Section II A. Hyperparameters are selected as NAdam optimizer, MAE loss, Glorot Uniform weight initializers, and tanh activation function for 4500 epochs and 32 batch size. It is seen from Figure 1, that the models with seven inputs make the highest predictions from test data, but when the predictions for exotic particles are examined, the models with 11 inputs give the highest predictions. Therefore we examined the losses of the training and test sets for possible overtraining for the data of 11 inputs, and there was no minor gap between training and test losses. Thus, one can safely conclude that 11-input models make good testing but poor exotic predictions. Finally, Figure 1 reveals that the 15-input data set suggested by Ref.[31] performs the best both for the exotic and the test set.

After determining the input size, the optimal values of the remaining hyperparameters are determined. Various optimizers have been experimented with and represented in Figure 2 that concludes Adam, NAdam, and Adamax optimizers perform similarly, while RMSProp results seem to be bad both for training and test sets.

A similar calculation has been carried out for the activation functions of the layers. Two different activation functions (ReLU and tanh) have been experimented with, and results are shown in Figure 3. The figure indicates that while the ReLU activation function gives successful outcomes for the test set, the predictions for the test set are higher than expected. The contrary of this comment is valid for the tanh activation function. Since the study's primary purpose is to make a successful mass estimation for exotic hadrons, tanh is chosen for the activation function.

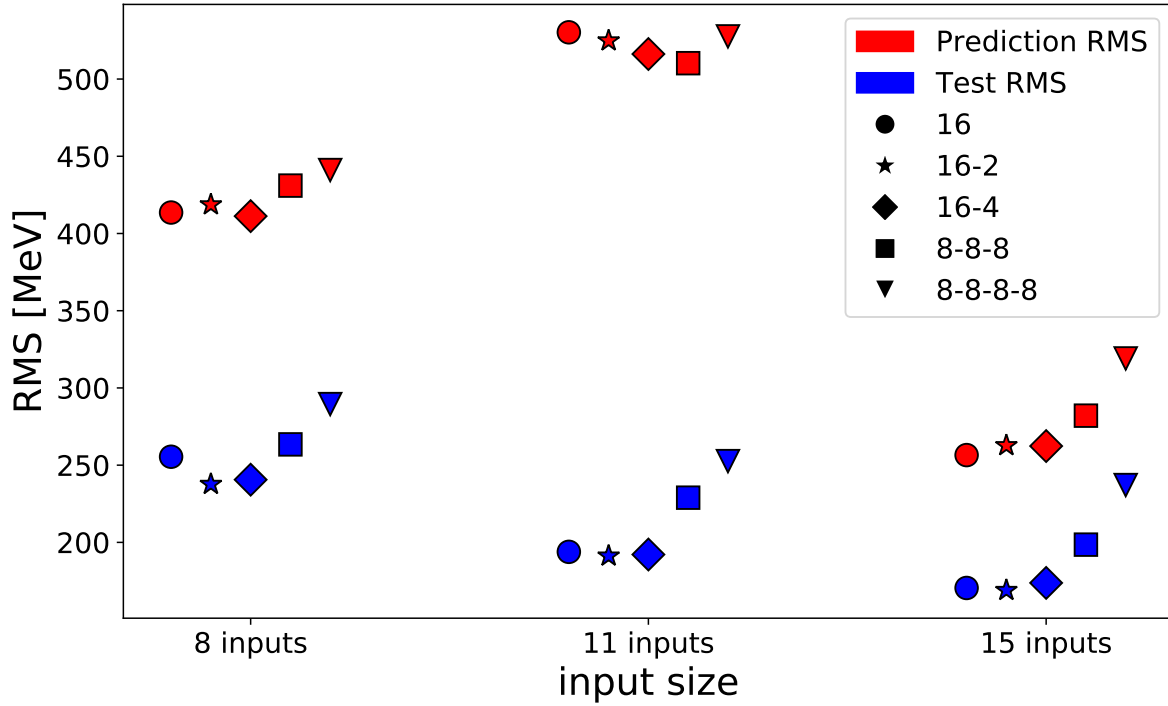


Figure 1: The root-mean-square errors for different input sizes. Blue colors represent errors from test sets; red colors represent prediction errors of exotic particles. Architectures are categorized by shapes. Hyperparameters are selected as NAdam optimizer, MAE loss, Glorot Uniform weight initializers, and tanh activation function for 4500 epochs and 32 batch size.

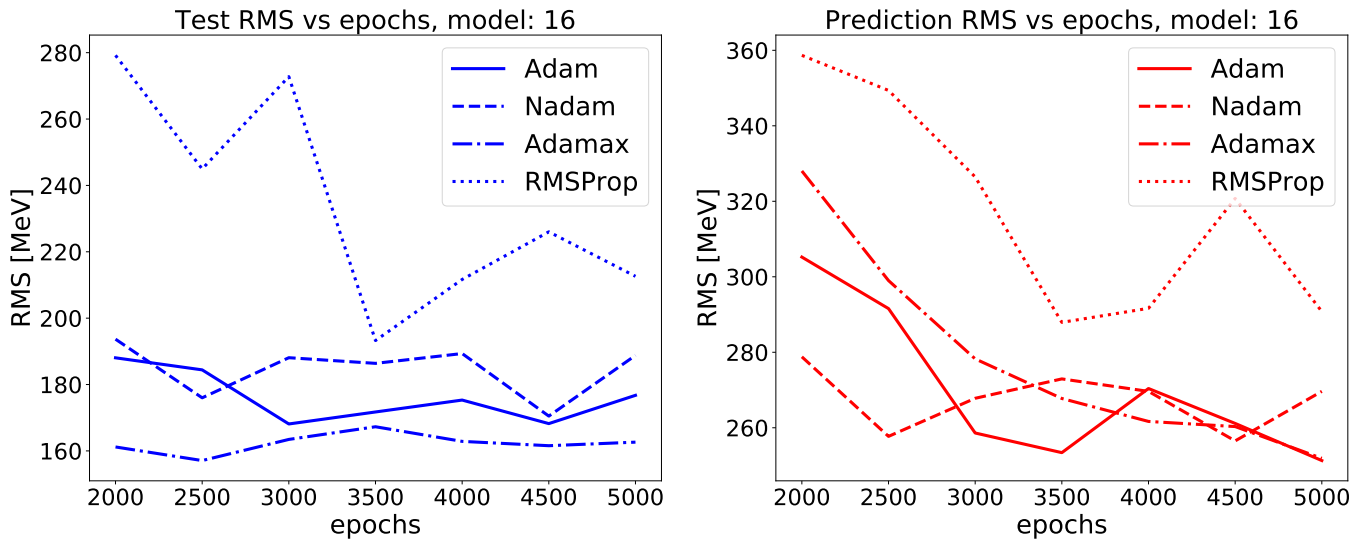


Figure 2: The root-mean-square errors for various epochs and optimizers. Blue colors represent errors from test sets, red colors represent prediction errors of exotic particles. Optimizers are categorized by linestyles. The comparison is performed for single hidden layer 16-node neural network. Remaining hyperparameters are selected as MAE loss, Glorot Uniform weight initializers, and tanh activation function for 32 batch size.

Later, the predictions are tried to be improved by using data augmentation techniques mentioned in the Section II C.

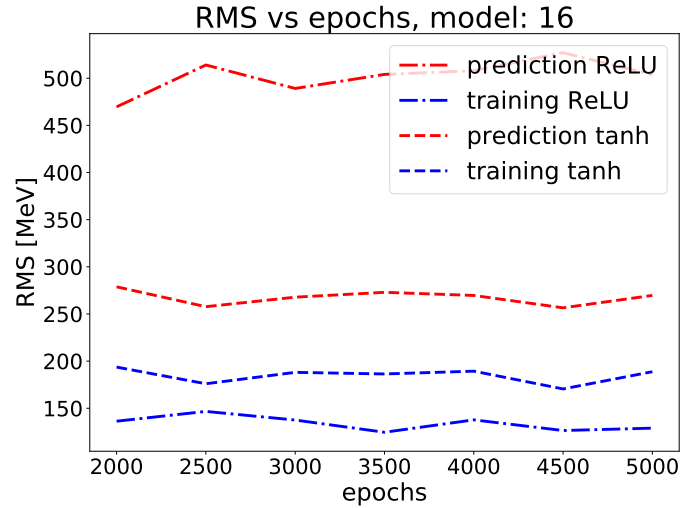


Figure 3: The root-mean-square errors for various epochs and activation. Blue colors represent errors from test sets, red colors represent prediction errors of exotic particles. Activations are categorized by linestyles. The comparison is performed for single hidden layer 16-node neural network. Remaining hyperparameters are selected as MAE loss, NAdam optimizer, Glorot Uniform weight initializers, and 32 batch size.

Two different types of data augmentation techniques have been performed. Firstly, data is increased from 2 to 10 times using Normal distribution. Next, the training data is doubled, where experimental errors are manually added. The best results are obtained with 15 inputs, NAdam optimizer, MAE loss, Glorot Uniform weight initializers, and tanh activation function. In order to minimize the fluctuations coming from randomness, experiments have been performed, and averages are taken using ten different seeds. All of the 5 architectures have been experimented, 16, 16 – 2, 16 – 4 architectures gave reasonably close results.

Architecture: 16, Loss:MAE, Optimizer:Nadam, Activation: tanh, epoch: 4500, batch: 32

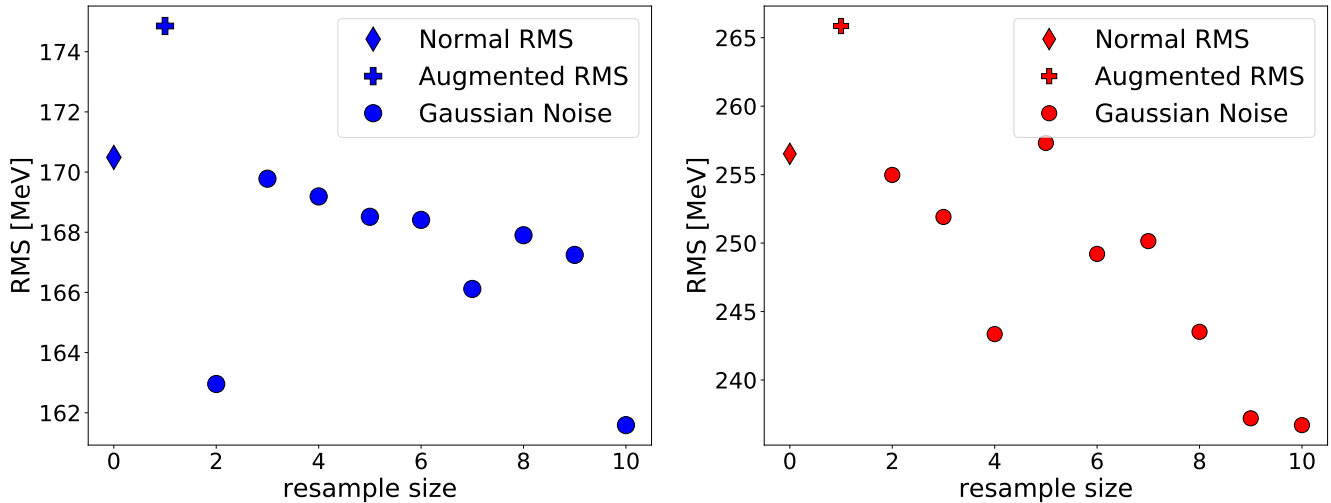


Figure 4: The root-mean-square errors for different resampling sizes. Blue colors represent errors from test sets, red colors represent prediction errors of exotic particles. Thin diamond represents non-augmented data. Plus represents manually augmented data. Filled circles represents resampling of normal distributon. The comparison is performed for single hidden layer 16-node neural network with MAE loss, NAdam optimizer, Glorot Uniform weight initializers, 4500 epochs and 32 batch size.

Figure 4 summarizes that the predictions are improved after artificially increasing the training data set. Although the number of data is limited, an improvement is observed around 5% in the test set and 8% in the prediction set.



The single-layer model (16) with Gaussian Noise of 9 times augmented is chosen for comparison.

Table I: Mass predictions for exotic hadrons (in units of MeV) along with a comparison to the Experimental [29] and other Neural Network (NN), Gaussian Process (GP), Constituent Quark Model results [31].

Hadron	$I, (J^P)$	Structure	Experiment [29]	This Work	NN [31]	GP [31]	CQM [31]
$X(3872)$	$0 (1^+)$	$c\bar{u}c\bar{u}$	$3871.69 \pm 0.17$	3828.19	$4815 \pm 786$	$3514 \pm 190$	3772
$Z_c(3900)$	$0 (1^+)$	$c\bar{d}\bar{c}u$	$3886.6 \pm 2.4$	4075.65	$4991 \pm 815$	$3515 \pm 199$	3776
$Z_c(4020)$	$0 (1^+)$	$c\bar{d}\bar{c}u$	$4024.1 \pm 1.9$	4297.87			
$Z_c(4430)$	$0 (1^+)$	$c\bar{d}\bar{c}u$	$4478_{-18}^{+15}$	4520.09			
$Y(4260)$	$0 (1^-)$	$c\bar{s}s\bar{c}$	$4230 \pm 8$	4049.13	$5400 \pm 1100$	$3543 \pm 1167$	4072
$Y(4360)$	$0 (1^-)$	$c\bar{u}c\bar{u}$	$4368 \pm 13$	3890.64	$4940 \pm 903$	$3107 \pm 168$	3772
$Y(4660)$	$0 (1^-)$	$u\bar{u}c\bar{c}$	$4643 \pm 9$	4112.86			
$P_c(4312)$	$\frac{1}{2} (\frac{1}{2}^+)$	$uudc\bar{c}$	$4311.9 \pm 0.7$	4171.04	$4200 \pm 1200$	$3544 \pm 923$	4112
$P_c(4440)$	$\frac{1}{2} (\frac{1}{2}^-)$	$uudc\bar{c}$	$4440.3 \pm 1.3$	4147.95	$4100 \pm 1100$	$3253 \pm 846$	
$P_c(4457)$	$\frac{1}{2} (\frac{3}{2}^-)$	$uudc\bar{c}$	$4457.3 \pm 0.6$	4365.89	$4500 \pm 1100$	$3581 \pm 932$	
$Z_b(100610)$	$0 (1^+)$	$b\bar{d}b\bar{u}$	$10607.2 \pm 2.0$	10403.09	$14700 \pm 1700$	$9907 \pm 560$	10136
$Z_b(100650)$	$0 (1^+)$	$b\bar{d}b\bar{u}$	$10652.2 \pm 1.5$	10570.77			

Recently a study has been performed to estimate baryon masses from meson masses using the Gaussian Process and neural networks and comparing the findings with the Constituent Quark Model [31]. The results from [31] along with our results are listed in Table I, it is clearly seen that Data Augmented neural networks could make successful predictions.

Afterward, predictions have been made for baryons, which existence predicted by the quark model but not experimentally observed yet. Predictions are made for spin- $\frac{1}{2}$   $\Omega_{cc}$  and spin- $\frac{3}{2}$   $\Omega_{cc}^*$  baryons in the  $c$  quark sector, and  $\Xi_{bb}$ ,  $\Omega_{bb}$  and their spin- $\frac{3}{2}$  partners in the bottomed quark sector. Finally, we also make a prediction for the recently experimentally observed baryon  $\Xi_{cc}$  in Table II.

Table II: Mass predictions for doubly charmed and bottomed baryons (in units of MeV) along with a comparison to the Lattice QCD or Experimental (only for  $\Xi_{cc}$  baryon) results.

Baryon	$I, (J^P)$	Structure	This Work	Lattice QCD or Experimental Results
$\Omega_{cc}$	$0, (\frac{1}{2}^+)$	$scc$	3713.17	$3704 \pm 17$ [33]
$\Omega_{cc}^*$	$0, (\frac{3}{2}^+)$	$scc$	3931.11	$3779 \pm 18$ [33]
$\Xi_{cc}$	$\frac{1}{2}, (\frac{1}{2}^+)$	$ucc$	3673.53	$3621 \pm 0.4$ [29]
$\Xi_{cc}^*$	$\frac{1}{2}, (\frac{3}{2}^+)$	$ucc$	3891.47	$3706 \pm 28$ [33]
$\Omega_{bb}$	$0, (\frac{1}{2}^+)$	$sbb$	10067.79	$10273 \pm 27 \pm 20$ [34]
$\Omega_{bb}^*$	$0, (\frac{3}{2}^+)$	$sbb$	10281.95	$10308 \pm 27 \pm 21$ [34]
$\Xi_{bb}$	$\frac{1}{2}, (\frac{1}{2}^+)$	$ubb$	10028.82	$10143 \pm 30 \pm 23$ [34]
$\Xi_{bb}^*$	$\frac{1}{2}, (\frac{3}{2}^+)$	$ubb$	10243.04	$10178 \pm 30 \pm 24$ [34]

Table II summarizes our results and compares them with Lattice QCD predictions. In the  $c$  quark sector, neural network results for spin- $\frac{3}{2}$  particles seem mildly higher than the lattice results. For the  $\Xi_{cc}$  baryon, the only experimentally observed particle in this table, the gap between Experiment and Networks prediction is only 2%. Finally, for the  $\Omega_{cc}$  baryon, Lattice and our prediction agree within errors. In the bottomed quark sector, Lattice and neural network predictions roughly agree. Except for  $\Omega_{bb}$ , which seems like 200 MeV gap is observed between predictions. Our findings show that increasing the training data set artificially improves predictions' success.

#### IV. DISCUSSION AND FUTURE WORKS

This study set out to implement neural networks to predict masses of exotic hadrons from ordinary hadrons (mesons and baryons). To this end, we use the total of 432 experimental data of mesons and baryons from the Particle Data Group as input. Three different input types are used to study the performance of this neural network predictions. It is observed that using categorical variables for quarks in the input layer increases the neural network's performance. The second aim of this study is to investigate the effects of data augmentation on the predictive power of neural network architectures. The experimental error values and the Gaussian augmentation techniques are used to increase the training data set artificially. After selecting the epoch and batch values, we performed ten calculations with different seeds to decrease the fluctuation from randomization.

This study has shown that data augmentation techniques play an essential role in improving neural network predictions. The neural networks can make reasonable predictions for exotic hadrons, doubly charmed and doubly bottomed baryons. The results are also comparable to other models. Although the limitation of this study is that neural networks does not include any theoretical physics approach behind them and are considered as a statistical model, the study has shown that the neural networks can make rapid and reliable predictions with a proper architecture; therefore, the neural networks might be used as an alternative tool.

Further research might explore exotic hadrons using Bayesian neural networks. Moreover, the neural network approaches can be used to train the residues of masses, which could be valuable to understanding the absent physics behind other models.

#### ACKNOWLEDGMENTS

The numerical calculations reported in this paper were partially performed at TÜBİTAK ULAKBİM, High Performance and Grid Computing Center (TRUBA resources).

- 
- [1] S. K. Choi, et al., Observation of a narrow charmonium-like state in exclusive  $b^\pm \rightarrow k^\pm \pi^+ \pi^- J/\psi$  decays, Phys. Rev. Lett. 91 (2003) 262001. [arXiv:hep-ex/0309032](https://arxiv.org/abs/hep-ex/0309032), [doi:10.1103/PhysRevLett.91.262001](https://doi.org/10.1103/PhysRevLett.91.262001).
- [2] A. Abulencia, et al., Analysis of the quantum numbers  $J^{PC}$  of the  $X(3872)$ , Phys. Rev. Lett. 98 (2007) 132002. [arXiv:hep-ex/0612053](https://arxiv.org/abs/hep-ex/0612053), [doi:10.1103/PhysRevLett.98.132002](https://doi.org/10.1103/PhysRevLett.98.132002).
- [3] S. K. Choi, et al., Bounds on the width, mass difference and other properties of  $X(3872) \rightarrow \pi^+ \pi^- J/\psi$  decays, Phys. Rev. D 84 (2011) 052004. [arXiv:1107.0163](https://arxiv.org/abs/1107.0163), [doi:10.1103/PhysRevD.84.052004](https://doi.org/10.1103/PhysRevD.84.052004).
- [4] P. del Amo Sanchez, et al., Evidence for the decay  $X(3872) \rightarrow J/\psi \omega$ , Phys. Rev. D 82 (2010) 011101. [arXiv:1005.5190](https://arxiv.org/abs/1005.5190), [doi:10.1103/PhysRevD.82.011101](https://doi.org/10.1103/PhysRevD.82.011101).
- [5] R. Aaij, et al., Determination of the  $X(3872)$  meson quantum numbers, Phys. Rev. Lett. 110 (2013) 222001. [arXiv:1302.6269](https://arxiv.org/abs/1302.6269), [doi:10.1103/PhysRevLett.110.222001](https://doi.org/10.1103/PhysRevLett.110.222001).
- [6] M. Ablikim, et al., Observation of a Charged Charmoniumlike Structure in  $e^+e^- \rightarrow \pi^+\pi^- J/\psi$  at  $\sqrt{s} = 4.26$  GeV, Phys. Rev. Lett. 110 (2013) 252001. [arXiv:1303.5949](https://arxiv.org/abs/1303.5949), [doi:10.1103/PhysRevLett.110.252001](https://doi.org/10.1103/PhysRevLett.110.252001).
- [7] A. Bondar, et al., Observation of two charged bottomonium-like resonances in  $Y(5S)$  decays, Phys. Rev. Lett. 108 (2012) 122001. [arXiv:1110.2251](https://arxiv.org/abs/1110.2251), [doi:10.1103/PhysRevLett.108.122001](https://doi.org/10.1103/PhysRevLett.108.122001).
- [8] R. Aaij, et al., Observation of  $J/\psi p$  Resonances Consistent with Pentaquark States in  $\Lambda_b^0 \rightarrow J/\psi K^- p$  Decays, Phys. Rev. Lett. 115 (2015) 072001. [arXiv:1507.03414](https://arxiv.org/abs/1507.03414), [doi:10.1103/PhysRevLett.115.072001](https://doi.org/10.1103/PhysRevLett.115.072001).
- [9] S. Gazula, J. Clark, H. Bohr, [Learning and prediction of nuclear stability by neural networks](https://arxiv.org/abs/1909.01911), Nuclear Physics A 540 (1) (1992) 1–26. [doi:https://doi.org/10.1016/0375-9474\(92\)90191-L](https://doi.org/10.1016/0375-9474(92)90191-L).  
URL <https://www.sciencedirect.com/science/article/pii/037594749290191L>
- [10] S. Athanassopoulos, E. Mavrommatis, K. Gernoth, J. Clark, [Nuclear mass systematics using neural networks](https://arxiv.org/abs/nucl-th/0408006), Nuclear Physics A 743 (4) (2004) 222–235. [doi:https://doi.org/10.1016/j.nuclphysa.2004.08.006](https://doi.org/10.1016/j.nuclphysa.2004.08.006).  
URL <https://www.sciencedirect.com/science/article/pii/S0375947404008632>
- [11] R.-D. Lasserri, D. Regnier, J.-P. Ebran, A. Penon, [Taming nuclear complexity with a committee of multilayer neural networks](https://arxiv.org/abs/2005.16250), Phys. Rev. Lett. 124 (2020) 162502. [doi:10.1103/PhysRevLett.124.162502](https://doi.org/10.1103/PhysRevLett.124.162502).  
URL <https://link.aps.org/doi/10.1103/PhysRevLett.124.162502>
- [12] E. Yüksel, D. Soydaner, H. Bahtiyar, Nuclear binding energy predictions using neural networks: Application of the multilayer perceptron, Int. J. Mod. Phys. E 30 (03) (2021) 2150017. [arXiv:2101.12117](https://arxiv.org/abs/2101.12117), [doi:10.1142/S0218301321500178](https://doi.org/10.1142/S0218301321500178).
- [13] D. Guest, K. Cranmer, D. Whiteson, Deep Learning and its Application to LHC Physics, Ann. Rev. Nucl. Part. Sci. 68 (2018) 161–181. [arXiv:1806.11484](https://arxiv.org/abs/1806.11484), [doi:10.1146/annurev-nucl-101917-021019](https://doi.org/10.1146/annurev-nucl-101917-021019).
- [14] A. Radovic, M. Williams, D. Rousseau, M. Kagan, D. Bonacorsi, A. Himmel, A. Aurisano, K. Terao, T. Wongjirad, Machine learning at the energy and intensity frontiers of particle physics, Nature 560 (7716) (2018) 41–48. [doi:10.1038/s41586-018-0361-2](https://doi.org/10.1038/s41586-018-0361-2).



- [15] R. Aaij, et al., The lhcb trigger and its performance in 2011, JINST 8 (2013) P04022. doi:[10.1088/1748-0221/8/04/P04022](https://doi.org/10.1088/1748-0221/8/04/P04022).
- [16] H. Luo, M.-x. Luo, K. Wang, T. Xu, G. Zhu, Quark jet versus gluon jet: fully-connected neural networks with high-level features, Sci. China Phys. Mech. Astron. 62 (9) (2019) 991011. arXiv:[1712.03634](https://arxiv.org/abs/1712.03634), doi:[10.1007/s11433-019-9390-8](https://doi.org/10.1007/s11433-019-9390-8).
- [17] J. Renner, et al., Background rejection in NEXT using deep neural networks, JINST 12 (01) (2017) T01004. doi:[10.1088/1748-0221/12/01/T01004](https://doi.org/10.1088/1748-0221/12/01/T01004).
- [18] D. R. Parisi, M. C. Mariani, M. A. Laborde, Solving differential equations with unsupervised neural networks, Chemical Engineering and Processing: Process Intensification 42 (8) (2003) 715–721. doi:[https://doi.org/10.1016/S0255-2701\(02\)00207-6](https://doi.org/10.1016/S0255-2701(02)00207-6).  
URL <https://www.sciencedirect.com/science/article/pii/S0255270102002076>
- [19] H. Mutuk, A study of excited  $\Omega_b^-$  states in hypercentral constituent quark model via artificial neural network, Eur. Phys. J. A 56 (5) (2020) 146. doi:[10.1140/epja/s10050-020-00161-5](https://doi.org/10.1140/epja/s10050-020-00161-5).
- [20] M. Sugawara, Numerical solution of the schrödinger equation by neural network and genetic algorithm, Computer Physics Communications 140 (3) (2001) 366–380. doi:[https://doi.org/10.1016/S0010-4655\(01\)00286-7](https://doi.org/10.1016/S0010-4655(01)00286-7).  
URL <https://www.sciencedirect.com/science/article/pii/S0010465501002867>
- [21] P. E. Shanahan, D. Trewartha, W. Detmold, Machine learning action parameters in lattice quantum chromodynamics, Phys. Rev. D 97 (9) (2018) 094506. arXiv:[1801.05784](https://arxiv.org/abs/1801.05784), doi:[10.1103/PhysRevD.97.094506](https://doi.org/10.1103/PhysRevD.97.094506).
- [22] B. Yoon, T. Bhattacharya, R. Gupta, Machine Learning Estimators for Lattice QCD Observables, Phys. Rev. D 100 (1) (2019) 014504. arXiv:[1807.05971](https://arxiv.org/abs/1807.05971), doi:[10.1103/PhysRevD.100.014504](https://doi.org/10.1103/PhysRevD.100.014504).
- [23] S. Y. Chen, H. T. Ding, F. Y. Liu, G. Papp, C. B. Yang, Machine learning spectral functions in lattice QCD (10 2021). arXiv:[2110.13521](https://arxiv.org/abs/2110.13521).
- [24] A. Krizhevsky, I. Sutskever, G. Hinton, Imagenet classification with deep convolutional neural networks, Advances in Neural Information Processing Systems (2012) 1097–1105.
- [25] H. A., P. Norvig, F. Pereira, The unreasonable effectiveness of data, IEEE Intelligent Systems 24 (2009) 8–12.
- [26] B. M., B. E., Scaling to very very large corpora for natural language disambiguation, Proceedings of the 39th annual meeting of the Association for Computational Linguistics (2001) 26–33.
- [27] H. Bahtiyar, D. Soydaner, E. Yüksel, Application of multilayer perceptron with data augmentation in nuclear physics, Applied Soft Computing In Press. arXiv:[2205.07953](https://arxiv.org/abs/2205.07953), doi:<https://doi.org/10.1016/j.asoc.2022.109470>.
- [28] C. M. Bishop, Neural Networks for Pattern Recognition, Oxford University Press, Inc., USA, 1995.
- [29] P. A. Zyla, et al., Review of Particle Physics, PTEP 2020 (8) (2020) 083C01. doi:[10.1093/ptep/ptaa104](https://doi.org/10.1093/ptep/ptaa104).
- [30] E. Rodrigues, B. Krikler, C. Burr, D. Smirnov, H. Dembinski, H. Schreiner, J. Nandi, J. Pivarski, M. Feickert, M. Marinangeli, et al., The scikit hep project overview and prospects, in: EPJ Web of Conferences, Vol. 245, EDP Sciences, 2020, p. 06028.
- [31] Y. Gal, V. Jejjala, D. K. Mayorga Peña, C. Mishra, Baryons as solitons in the meson spectrum: A machine learning perspective, Int. J. Mod. Phys. A 37 (06) (2022) 2250031. doi:[10.1142/S0217751X22500312](https://doi.org/10.1142/S0217751X22500312).
- [32] Y. Goodfellow I., Bengio, Deep Learning, From Adaptive Computation and Machine Learning series, MIT Press, 2016.  
URL <https://mitpress.mit.edu/books/deep-learning>
- [33] Y. Namekawa, et al., Charmed baryons at the physical point in 2+1 flavor lattice qcd, Phys. Rev. D 87 (9) (2013) 094512. arXiv:[1301.4743](https://arxiv.org/abs/1301.4743), doi:[10.1103/PhysRevD.87.094512](https://doi.org/10.1103/PhysRevD.87.094512).
- [34] Z. S. Brown, W. Detmold, S. Meinel, K. Orginos, Charmed bottom baryon spectroscopy from lattice QCD, Phys. Rev. D 90 (9) (2014) 094507. arXiv:[1409.0497](https://arxiv.org/abs/1409.0497), doi:[10.1103/PhysRevD.90.094507](https://doi.org/10.1103/PhysRevD.90.094507).